Ultrasensitive detection of porcine circovirus type 2 using gold(III) enhanced chemiluminescence immunoassay

Huimin Zhang,[a] Wentao Li,[b] Zonghai Sheng,[a] Heyou Han*[a] and Qigai He*[b]

Porcine circovirus type 2 (PCV2) is associated with many diseases especially postweaning multisystemic wasting syndrome (PMWS), which has brought huge economic loss to the swine industry worldwide. Viral detection will pave the way for this disease prevention. Herein, we developed a facile, rapid and ultrasensitive method for detection of PCV2 based on gold(III) enhanced chemiluminescence immunoassay (CLIA). The gold(III), dissolved from the gold nanoparticle–monoclonal antibody conjugate, served as an analyte for the indirect measurement of PCV2. Under the optimal conditions, the detection limit for the detection of PCV2 was 1.71×10^3 copies mL^{-1}. Moreover, the CLIA signal can be further enhanced by using hydroxylamine-amplified gold nanoparticles, and the limit of detection was as low as 2.67×10^2 copies mL^{-1}. Compared with conventional polymerase chain reaction (PCR), the proposed method has good sensitivity and reliability in analysis of 36 serum samples, and showed great potential in virus assays.

Introduction

Animal diseases can not only cause huge economic loss, but also endanger human health. However, compared with human diseases, animal diseases have not attracted much attention. Porcine circovirus (PCV), which is classified in a newly recognized virus family—Circoviridae,[1] is a small non-enveloped virus with a single-stranded circular DNA genome of about 1.76 kb and a size of 17 nm in diameter.[2] At the 20th International Pig Veterinary Society Congress in 2008, PCV-associated disease was listed as the first disease which threaten the development of the swine industry. Two species of PCV have been characterized and are subsequently known as porcine circovirus type 1 (PCV1) and porcine circovirus type 2 (PCV2).[3] PCV1 is considered to be nonpathogenic to pigs by experimental inoculation. Increasing evidence indicate that PCV2 is the causative agent of the post-weaning multisystemic wasting syndrome (PMWS), porcine respiratory disease complex (PRDC) and porcine dermatitis and nephropathy syndrome (PDNS).[4–6] With the development of large-scale swine industry, the diseases caused by PCV2 are increasing, which have brought huge economic loss to the swine industry around the world. Now, most common methods for detection of PCV2 are biological methods. Analytical chemistry methods have rarely been reported and not gained the attention from chemical scientists. At present, PMWS is most commonly diagnosed with the detection of the antibody against PCV2, using enzyme-linked immunosorbent assay (ELISA), indirect immunofluorescence assay (IFA) and immunoperoxidase monolayer assay (IPMA).[7–12] However, whether the animals have been sick can be more directly proved by the viral detection. Until now, PCV2 serving as antigen for detection of PCV2 within an immunological method has rarely been reported. The mainly used methods for detection of PCV2 are various kinds of polymerase chain reaction (PCR).[13,14] But these methods have some limits, such as high cost, high false positive frequency, relatively long analysis time and requires sophisticated instrumentation. Therefore, developing a new method has great significance in the early detection of PCV2.

Chemiluminescence immunoassay (CLIA) offers both the advantages of chemiluminescence (CL) and immunoassay (IA), and it has been applied in clinical chemistry and bioanalysis.[15–19] Recently, nanomaterials serving as bioanalytical markers, especially gold nanoparticles, have attracted considerable interest because of their rapid and simple chemical synthesis, easy conjugation with biomolecules, good biocompatibility and stability.[16,19–27] Moreover, lower detection limits can be obtained by indirect detection of gold(III). However, CLIA based on gold(III) has rarely been used in detecting animal disease markers in recent years.[28] In our previous work, we reported an indirect fluorescence immunoassay for high-throughput screening of *Actinobacillus pleuroneumoniae* (APP) based on the fluorescence quenching of quantum dots by gold(III).[29] In this article, we report an ultrasensitive, simple, rapid, specific, and reproducible method for the detection of PCV2 using gold(III) enhanced CLIA. The limit of detection (LOD) was 2.67×10^2 copies mL^{-1}. In comparison with PCR, CLIA provided a great promising future for ultrasensitive and reliable detection of PCV2 in clinical analysis and controlling the transmission of the disease.

Experimental

Apparatus

Transmission electron microscope images (TEM, H-7650, Hitachi, Japan) were used to characterize the particle size of PCV2,

[a]College of Science, State Key Laboratory of Agricultural Microbiology, Huazhong Agricultural University, Wuhan, 430070, P.R. China. E-mail: hyhan@mail.hzau.edu.cn; Fax: +86 27 87288246; Tel: +86 27 87288246
[b]College of Animal Science and Veterinary Medicine, State Key Laboratory of Agricultural Microbiology, Huazhong Agricultural University, Wuhan, 430070, P.R. China. E-mail: heqigai@yahoo.com; Fax: +86 27 87282608; Tel: +86 27 87286974

gold nanoparticles and gold nanoparticle–monoclonal antibody conjugate. The CL signal was detected by a BPCL ultra-weak CL analyzer (Institute of Biophysics Academic Sinica, Beijing, China). The ultraviolet and visible (UV-vis) absorption spectra were made with a Thermo Nicolet Corporation Model evolution 300 UV-vis spectrometer. The pH measurements were acquired on a Model pHS-3C meter (Shanghai Leici Equipment Factory, China).

Reagents

Polystyrene 96-well plates were obtained from Keqian Animal Biological Products Co., Ltd. (Wuhan, China) and used to perform the immunoreactions. Bovine serum albumin (BSA) was from German Roche Co. (Germany). $HAuCl_4 \cdot 4H_2O$ was obtained from Shanghai Chemical Reagent Co. (Shanghai, China). The luminol stock solution (1.0×10^{-2} M) was prepared by dissolving luminol (obtained from Sigma) in 0.1 M NaOH solution and stored at 4 °C in a dark place. The buffers used were as follows: (A) coating buffer, 0.1 M sodium phosphate buffered saline (PBS), pH 7.2–7.4; (B) washing buffer, buffer A with 0.1% Tween 20. The monoclonal antibodies, standard positive and negative serum saved by our laboratory. Clinical serum samples were obtained from naturally infected and non-infected pigs. All chemical reagents were of analytical grade and the water was prepared by Milli-Q equipment and used throughout.

Preparation of gold nanoparticles and gold nanoparticle–monoclonal antibody conjugate

Gold nanoparticles were synthesized according to the method of Yu et al.[22] using citrate to reduce $HAuCl_4$. All glassware was soaked in highly concentrated HNO_3–HCl mixed solution for a time, then it was washed with water and dried before use. Firstly, 100 mL of 0.01% $HAuCl_4 \cdot 4H_2O$ solution was heated to boiling, then quickly added to 4 mL of 1% sodium citrate solution with vigorous stirring. After the color changed from light yellow to brilliant red, the solution was no longer heated but

stirred for another 5 min to complete the reduction of the $HAuCl_4$, then cooled to room temperature and stored at 4 °C. The synthesized gold nanoparticles were used for the preparation of gold nanoparticle–monoclonal antibody conjugate.

Gold nanoparticle–monoclonal antibody conjugate was prepared with some modifications following procedure of Hu et al.[20] The monoclonal antibody (20% more than the minimum amount determined by a flocculation test) was added to 10 mL gold nanoparticles suspension (pH adjusted to 8.5 with 0.1 M K_2CO_3), then stirred and incubated at room temperature for 30 min. The conjugate was centrifuged at 10 000g for 30 min, then the soft sediment was resuspended with 1% BSA in buffer A and stored at 4 °C.

Procedures for the CLIA and hydroxylamine-amplified CLIA

The principle of CLIA and hydroxylamine-amplified CLIA are depicted in Scheme 1. PCV2 was used as antigen and it was characterized by TEM and metrically analyzed as 17 nm in average diameter (Fig. 1). Each well of the 96-well polystyrene microplate plate was coated with a series of dilution of standard positive serum in buffer A (100 μL), which was incubated
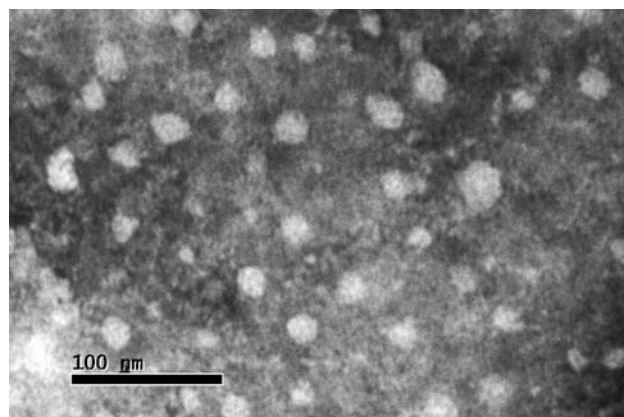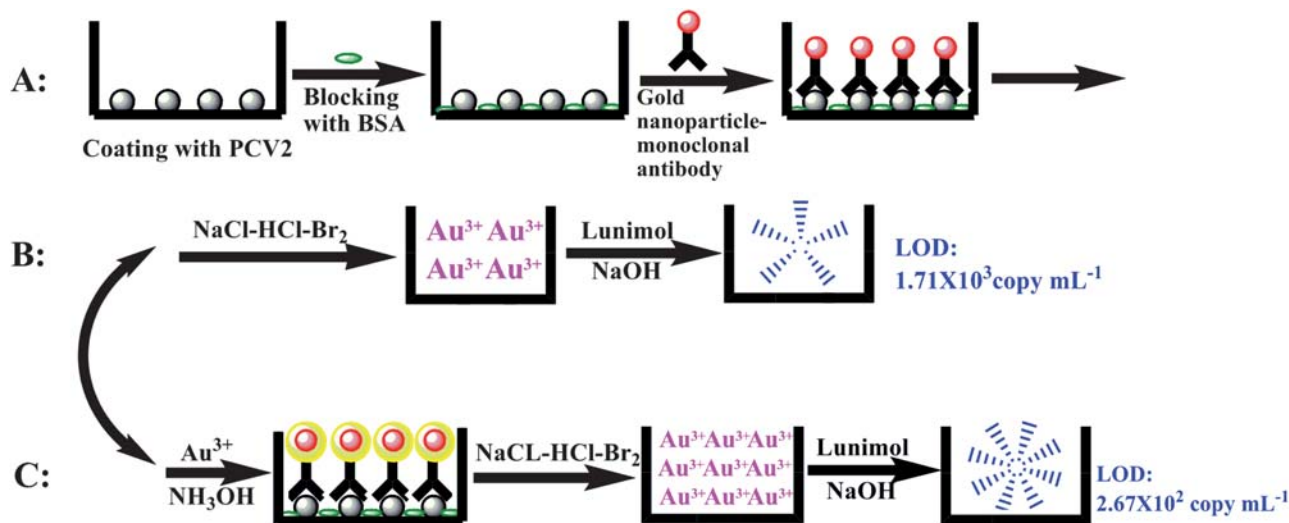

Fig. 1 TEM image of PCV2 using negative-staining method.

Scheme 1 Schematic representation of the Au nanoparticles-based CLIA and hydroxylamine-amplified CLIA. (A) Procedures for the immunoassay. (B) Procedures for conventional CL detection. (C) Procedures for hydroxylamine-amplified CL detection.

overnight at 4 °C. After removal of the unbound PCV2, each well of the plate was washed six times with buffer B. After that, the residual sites of each well was blocked with 300 µL 3% BSA in buffer A and incubated for 60 min at 37 °C. Then the wells were washed with buffer B six times, and 100 µL gold nanoparticle–monoclonal antibody conjugate was dispensed in each well. The wells were incubated at 37 °C for 60 min. Finally, each well of the plate was washed six times with buffer B.

For conventional CL detection, after removing the washing solution carefully, gold nanoparticles were dissolved with 1 mL per well of NaCl–HCl–Br$_2$ mixed solution for 20 min to ensure that the gold nanoparticles were dissolved to form AuCl$_4^-$ completely. The mixture was placed in the oven at 80 °C for 30 min to completely dry. After that 100 µL of the PBS was injected into each well and reacted for 10 min. Then 30 µL of the solution was transferred into glass tubes containing 1 mL 10^{-6} M luminol solution (dissolved in 0.1 M NaOH), and the CL signal was detected with the CL analyzer.

For hydroxylamine-amplified CL detection, after the wells were rinsed six times with buffer B, the gold nanoparticles which assembled on the surface of the 96-well plate were catalytically enlarged in the presence of 4.5 mM NH$_2$OH and 5 mM HAuCl$_4$ at 37 °C for 30 min. After the wells were washed three times with buffer B, the procedure for the detection of CL signal was similar to that described above.

Clinical sample detection and comparison with conventional PCR

The serum samples from infected pigs and non-infected pigs were subjected to analysis by our proposed method and PCR, respectively. The preparation of serum samples was as follows: Venous blood was taken from infected and non-infected pigs and stored at 37 °C for 60 min. The blood was centrifuged at 5000g for 10 min, and then the serum was collected for use. For PCR, the conditions are as follows. Amplification of PCV2 incorporated forward and reverse primers, F-PCV2 1092-5′ GTGCCTATAACATCAGGACCA and R-PCV2 1564′ CTGTCATATAGGCTTCCACGC, respectively. For PCR amplification, primers were used at a concentration of 2.5×10^{-7} M in a 25 µl reaction mixture containing master mix, sterile water, 1.5 µl of 2.5×10^{-2} M MgCl$_2$ and 2.5 µl of sample DNA. DNA was amplified using 35 cycles at 94 °C for 1 min, 54 °C for 1 min, and 72 °C for 1 min, followed by a 10 min extension at 72 °C. The PCR products were electrophoresed on a 1.0% agarose gel and visualized under UV light after staining with ethidium bromide.

Results and discussion

Characterization of gold nanoparticles and gold nanoparticle–monoclonal antibody conjugate

The UV-vis absorption spectra of gold nanoparticles and gold nanoparticle–monoclonal antibody conjugate were shown in Fig. 2. The gold nanoparticles exhibited a sharp plasmon absorption band with maximum absorbance at wavelength 519 nm due to the surface plasmon resonance, and the average particle size of as-prepared gold nanoparticles was 15 nm (curve a).[30] Because of the interaction of the monoclonal antibodies with gold nanoparticles, the surface plasmon band was
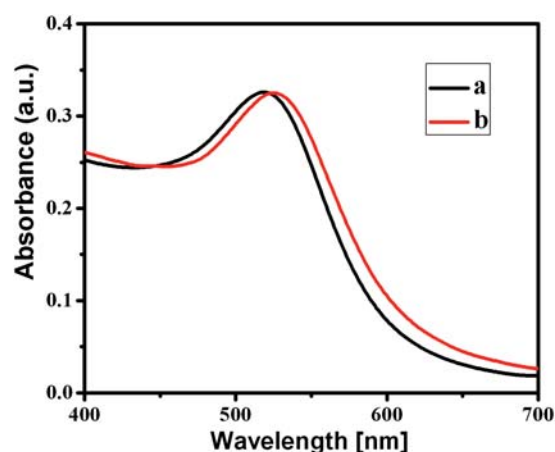

Fig. 2 UV-vis absorption spectra of (a) gold nanoparticles and (b) gold nanoparticle–monoclonal antibody conjugate.
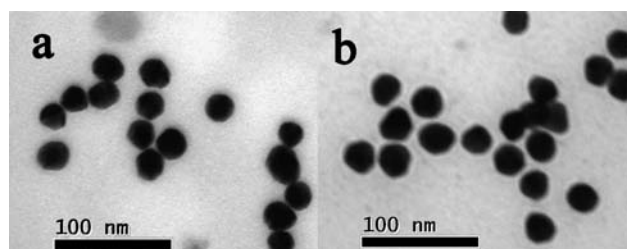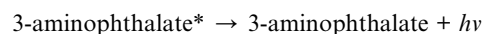

Fig. 3 TEM images of (a) gold nanoparticles and (b) gold nanoparticle–monoclonal antibody conjugate.

red-shifted after addition of the monoclonal antibody (curve b), which indicated the gold nanoparticle–monoclonal antibody conjugate was formed. The TEM image further verified the above results. As shown in Fig. 3, gold nanoparticles were on average 15 nm (Fig. 3a) in diameter and the gold nanoparticle–monoclonal antibody conjugate was 17 nm in diameter (Fig. 3b). The diameter of the nanoparticles increased 2 nm after the interaction of the monoclonal antibodys with gold nanoparticles. The results were consistent with that of UV-vis absorption spectra. The dispersity of the gold nanoparticle–monoclonal antibody conjugate was symmetrical and single.

Optimization of the CL conditions

Several parameters were studied systematically in order to establish optimal conditions for the CL detection of PCV2, including the concentrations of NaCl–HCl–Br$_2$ mixed solution, NaOH solution and luminol solution. The CLIA for determination of PCV2 is based on the catalytic effect of AuCl$_4^-$ on the luminol–NaOH system. The possible experimental principle for AuCl$_4^-$ enhanced CL intensity on the luminol–NaOH system can be illustrated as follows:[20]

$$AuCl_4^- + luminol \rightarrow AuCl_2^- + \text{3-aminophthalate*}$$

$$\text{3-aminophthalate*} \rightarrow \text{3-aminophthalate} + hv$$

AuCl$_4^-$ would speed up the electron transfer of luminol to yield 3-aminophthalate excited state and produced AuCl$_2^-$. The

state of excited 3-aminophthalate returns to the ground state with increased CL intensity. Therefore, it is the primary step to dissolve the gold nanoparticles from the gold nanoparticle–monoclonal antibody conjugate to form $AuCl_4^-$. This was achieved with the use of NaCl–HCl–Br_2 mixed solution. Clearly, the dissolution of gold nanoparticles in NaCl–HCl–Br_2 mixed solution can be affected by several factors including the concentrations of HCl, NaCl and Br_2. First, as shown in Fig. 4, the CL intensity increased with the increasing of NaCl concentration from 5.0×10^{-3} to 1.5×10^{-2} M, and then decreased. Therefore, 1.5×10^{-2} M NaCl was chosen as the optimum concentration for the CLIA. Second, as shown in Fig. 5, as the concentration of HCl increased, the CL intensity increased between 1.0×10^{-3} M and 7.0×10^{-2} M, and then maintained almost the same

Fig. 6 CL intensity *vs.* the concentration of Br_2. Experimental conditions: 50 µL gold nanoparticles (15 nm) was dissolved in 50 µL of NaCl-HCl–Br_2 solution (final concentration, 7×10^{-2} M HCl–1.5×10^{-2} M NaCl–different concentrations of Br_2), and then 30 µL of the resultant solution was injected into glass tubes containing 1.0×10^{-6} M luminol (dissolved in 0.1 M NaOH) for CL measurement.
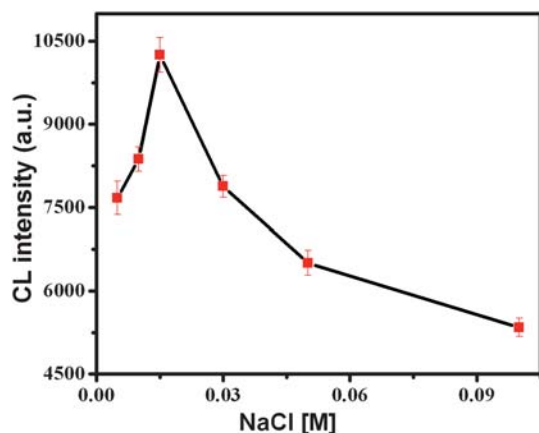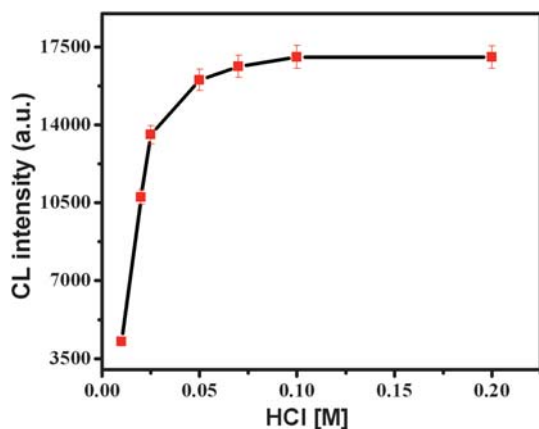

Fig. 4 CL intensity *vs.* the concentration of NaCl. Experimental conditions: 50 µL gold nanoparticles (15 nm) was dissolved in 50 µL of NaCl–HCl–Br_2 solution (final concentration, different concentrations of NaCl–0.1 M HCl–0.5×10^{-3} M Br_2), and then 30 µL of the resultant solution was injected into glass tubes containing 1.0×10^{-6} M luminol (dissolved in 0.1 M NaOH) for CL measurement.
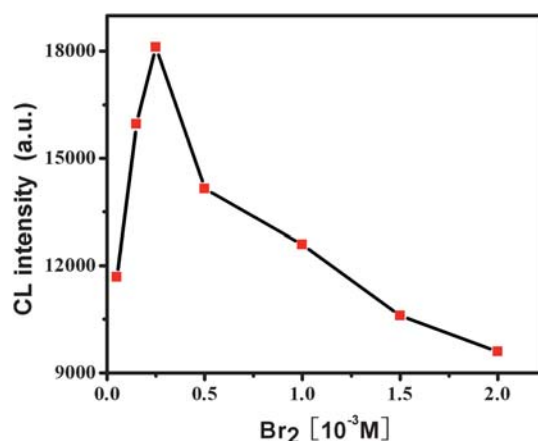
concentration in the range of 5.0×10^{-2} to 1.0×10^{-1} M HCl. Thus, 7.0×10^{-2} M HCl was selected for the following experiments. Third, as shown in Fig. 6, the CL intensity increased with increasing the concentration of Br_2 and reached a maximum value at 2.5×10^{-4} M. On the other hand, the CL intensity decreased when the concentration of Br_2 was higher than 2.5×10^{-4} M. Hence, subsequent work employed 2.5×10^{-4} M Br_2.

The CLIA is based on the catalytic effect of $AuCl_4^-$ on the luminol–NaOH CL reaction. In order to obtain reproducible and sensitive data, optimum concentrations of NaOH and luminol on the CL intensity were studied. The effect of NaOH concentration on the CL intensity was studied from the range of 8.0×10^{-3} to 2.0 M. It was found that CL intensity reached its maximum when the concentration of NaOH was 0.1 M (Fig. 7). Thus, 0.1 M NaOH was selected for subsequent work. The effect of the
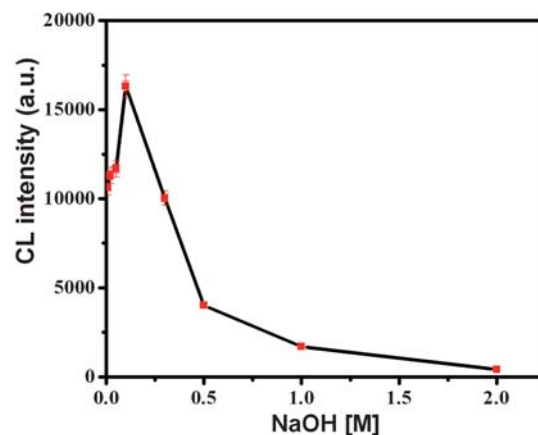

Fig. 5 CL intensity *vs.* the concentration of HCl. Experimental conditions: 50 µL gold nanoparticles (15 nm) was dissolved in 50 µL of NaCl–HCl–Br_2 solution (final concentration, different concentrations of HCl–1.5×10^{-2} M NaCl–0.5×10^{-3} M Br_2), and then 30 µL of the resultant solution was injected into glass tubes containing 1.0×10^{-6} M luminol (dissolved in 0.1 M NaOH) for CL measurement.

Fig. 7 CL intensity *vs.* the concentration of NaOH. Experimental conditions: 50 µL gold nanoparticles (15 nm) was dissolved in 50 µL of HCl–NaCl–Br_2 solution (final concentration, 7.0×10^{-2} M HCl–1.5×10^{-2} M NaCl–2.5×10^{-4} M Br_2), and then 30 µL of the resultant solution was injected into glass tubes containing 1.0×10^{-6} M luminol solution (dissolved in different concentrations of NaOH) for CL measurement.
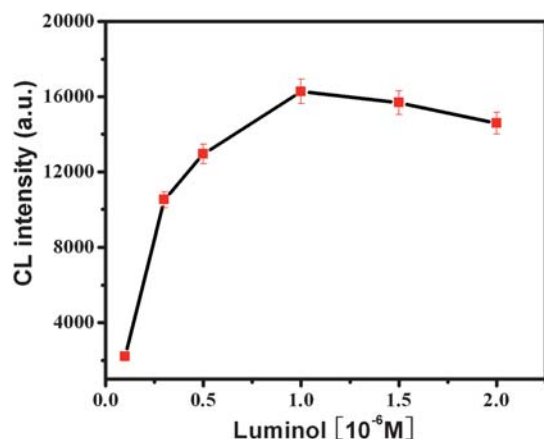
Fig. 8 CL intensity *vs.* the concentration of luminol. Experimental conditions: 50 µL of gold nanoparticles (15 nm) was dissolved in 50 µL of HCl–NaCl–Br$_2$ solution (final concentration, 7.0×10^{-2} M HCl–1.5×10^{-2} M NaCl–2.5×10^{-4} M Br$_2$), and then 30 µL of the resultant solution was injected into glass tubes containing different concentrations of luminol (dissolved in 0.1 M NaOH) for CL measurement.

concentration of luminol on the CL intensity was investigated. The results showed that the CL intensity increased from the range of 1.0×10^{-7} to 1.0×10^{-6} M as the increasing of luminol concentration, and maintained almost the same in the range of 1.0×10^{-6} to 2.0×10^{-6} M luminol (Fig. 8). Hence, 1.0×10^{-6} M luminol was selected for the following experiments.

CLIA for detection of PCV2

The analytical performance based on luminol–NaOH–AuCl$_4^-$ CL system was assessed by measuring the CL intensity upon the concentration of PCV2. Under the optimized experimental conditions, the relationship between the CL intensity and different concentration of PCV2 (standard positive serum) was investigated. A good calibration graph in the amount range of 5.12×10^3–1.60×10^7 copy mL^{-1} showed a linear correlation ($r = 0.9910$) between the logarithm of the concentration of the PCV2 and the CL intensity, represented by $I = 595.14C + 3913.94$ (I is the CL intensity and C is logarithm of the concentration of PCV2) (Fig. 9). The LOD was 1.71×10^3 copy mL^{-1}.
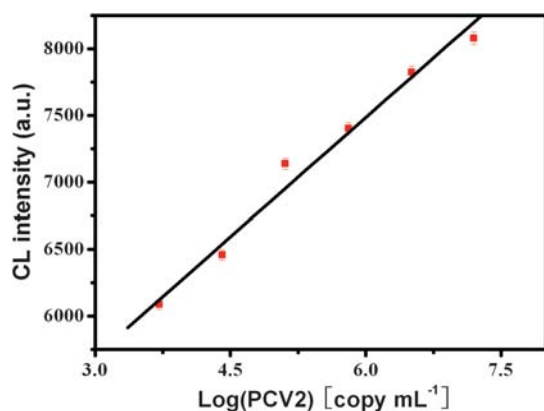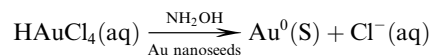
For hydroxylamine-amplified gold nanoparticles, the reaction is as follows:

$$HAuCl_4(aq) \xrightarrow[\text{Au nanoseeds}]{NH_2OH} Au^0(S) + Cl^-(aq)$$

This reaction is accelerated dramatically on the surface of colloidal gold nanoseeds. Thousands of gold atoms are contained in each gold nanoparticle (*e.g.*, 15 nm spherical gold nanoparticle theoretically contains 1.10×10^5 gold atoms).[30] Thus, after the hydroxylamine amplification, more AuCl$_4^-$ can be dissolved by NaCl–HCl–Br$_2$ solution. The CLIA is based on the AuCl$_4^-$ enhanced luminol CL reaction, so hydroxylamine-amplified gold nanoparticles can improve the sensitivity of the CL reaction. As shown in Fig. 10, under the optimized experimental conditions, the CL intensity was linear with the logarithm of the concentration of PCV2 in the range from 8.00×10^2 copy mL^{-1} to 8.00×10^7 copy mL^{-1}. The regression equation was $I = 1064.45C + 2450.03$ (I is the CL intensity and C is logarithm of the concentration of PCV2) with a good linear correlation ($r = 0.9942$). As low as 2.67×10^2 copy mL^{-1} could be sensitively detected using this method, which is lower than the conventional CL detection limit. This method offers great promise for highly sensitive detection of other animal disease markers.

Clinical samples detection

To evaluate the diagnostic performance of the CLIA, 36 clinical serum samples were analyzed by the proposed method and PCR, respectively. PCR has been recognized as a sensitive and specific method used in detection of PCV2. As shown in Table 1, compared with PCR, CLIA showed good results: high efficiency (88.9%), high sensitivity (95%), high specificity (81.3%), moderate false-positive rate (18.8%) and low false-negative rate (5.0%). Among 36 clinical serum samples, 22 serum were positive in CLIA and positive rate was 61.1% while 20 serum samples were positive in PCR and positive rate was 55.6%. Among 22 positive serum samples in CLIA, 19 serum were positive in PCR, while among 14 negative serum samples in CLIA, 13 serum samples were negative in PCR. Therefore, a high percentage of agreement (88.9%) was found between CLIA and PCR.
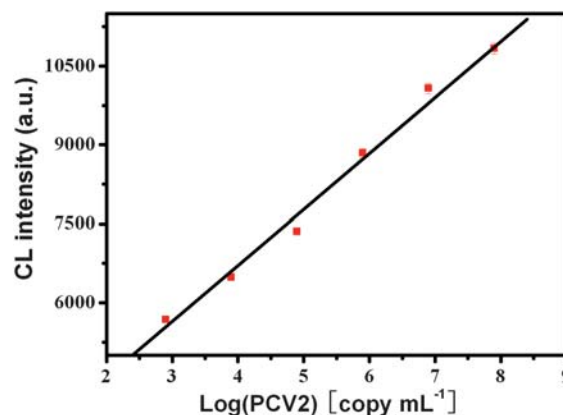

Fig. 9 Curve of CL intensity *versus* the logarithm of the concentration of PCV2.

Fig. 10 Curve of CL intensity *versus* the logarithm of the concentration of PCV2.

Table 1 Comparative results of the CLIA and PCR for detection of PCV2

		PCR			Performance				
		Positive	Negative	Total	Efficiency[a] (%)	Sensitivity[b] (%)	Specificity[c] (%)	FP rate[d] (%)	FN rate[e] (%)
CLIA	Positive	19	3	22					
	Negative	1	13	14	88.9	95.0	81.3	18.8	5.0
	Total	20	16	36					

[a] Efficiency = (TP + TN) × 100/Total. [b] Sensitivity = TP × 100/(TP + FN). [c] Specificity = TN × 100/(TN + FP). [d] False-positive rate = FP ×100/(FP + TN). [e] False-negative rate = FN × 100/(TP + FN). TP = True Positive. TF = True Negative.

Compared with PCR, our present CLIA provides remarkable advantages in terms of reliability and in practical uses, such as high sensitivity and specificity.

Conclusions

In summary, we take advantage of CL and IA to develop a CLIA method based on gold(III) enhanced luminol CL reaction for ultrasensitive detection of PCV2 in pig serum samples. This novel method offers several advantages such as high sensitivity, high specificity, simple operation, low cost, no radiation and easy automatization. The detection limit of PCV2 was 2.67×10^2 copy mL^{-1}. This is the first report for measuring PCV2 using hydroxylamine-amplified CLIA method, which showed great potential for numerous applications in immunoassay. At the clinical point of view, this method can be easily applied to the detection of other animal diseases and zoonosis. Furthermore, this technology can be developed to other metal nanoparticles as a marker. We believe that the method is of momentous current significance and far-reaching analytic significance in preventing, detecting, and controlling animal-borne disease outbreaks.

Acknowledgements

References

1 C. R. Pringle, *Arch. Virol.*, 1999, **144**, 2065.
2 I. Tischer, H. Gelderblom, W. Vettermann and M. A. Koch, *Nature*, 1982, **295**, 64.
3 G. M. Allan, F. McNeilly, S. Kennedy, B. Daft, E. G. Clarke, J. A. Ellis, D. M. Haines, B. M. Meehan and B. M. Adair, *J. Vet. Diagn. Invest.*, 1998, **10**, 3.
4 C. Chae, *Vet. J.*, 2005, **169**, 326.
5 J. Ellis, S. Krakowka, M. Lairmore, D. Haines, A. Bratanich, E. Clark, G. Allan, C. Konoby, L. Hassard, B. Meehan, K. Martin, J. Harding, S. Kennedy and F. McNeilly, *J. Vet. Diagn. Invest.*, 1999, **11**, 3.
6 J. Choi, G. W. Stevenson, M. Kiupel, B. Harrach, L. Anothayanontha, C. L. Kanitz and S. K. Mittal, *Can. J. Vet. Res.*, 2002, **66**, 217.
7 P. Nawagitgul, P. A. Harms, I. Morozov, B. J. Thacker, S. D. Sorden, C. Lekcharoensuk and P. S. Paul, *Clin. Diagn. Lab. Immunol.*, 2002, **9**, 33.
8 P. Blanchard, D. Mahé, R. Cariolet, C. Truong, M. L. Dimna, C. Arnauld, N. Rose, E. Eveno, E. Albina, F. Madec and A. Jestin, *Vet. Microbiol.*, 2003, **94**, 183.
9 I. W. Walker, C. A. Konoby, V. A. Jewhurst, I. McNair, F. McNeilly, B. M. Meehan, T. S. Cottrell, J. A. Ellis and G. M. Allan, *J. Vet. Diagn. Investig.*, 2000, **12**, 400.
10 S. B. Shang, Y. F. Li, J. Q. Guo, Z. T. Wang, Q. X. Chen, H. G. Shen and J. Y. Zhou, *Res. Vet. Sci.*, 2008, **84**, 150.
11 G. M. Allan, F. McNeilly, I. W. Walker, J. A. Young, A. J. Douglas and B. M. Adair, *Vet. Rec.*, 1998, **142**, 8.
12 D. J. Lefebvre, S. Costers, J. V. Doorsselaere, G. Misinzo, P. L. Delputte and H. J. Nauwynck, *J. Gen. Virol.*, 2008, **89**, 177.
13 K. S. Lyoo, H. B. Kim and H. S. Joo, *J. Vet. Diagn. Invest.*, 2008, **20**, 283.
14 Q. Liu, L. Wang, P. Willson and L. A. Babiuk, *J. Clin. Microbiol.*, 2000, **38**, 3474.
15 L. X. Zhao, L. Sun and X. G. Chu, *TrAC, Trends Anal. Chem.*, 2009, **28**, 404.
16 C. F. Duan, Y. Q. Yu and H. Cui, *Analyst*, 2008, **133**, 1250.
17 T. Matsunaga, M. Kawasaki, X. Yu, N. Tsujimura and N. Nakamura, *Anal. Chem.*, 1996, **68**, 3551.
18 M. H. Yang, Y. Kostov, H. A. Bruck and A. Rasooly, *Anal. Chem.*, 2008, **80**, 8532.
19 A. P. Fan, C. Lau and J. Z. Lu, *Anal. Chem.*, 2005, **77**, 3238.
20 D. H. Hu, H. Y. Han, R. Zhou, F. Dong, W. C. Bei, F. Jia and H. C. Chen, *Analyst*, 2008, **133**, 768.
21 Q. Dai, X. Liu, J. Coutts, L. Austin and Q. Huo, *J. Am. Chem. Soc.*, 2008, **130**, 8138.
22 Z. F. Peng, Z. P. Chen, J. H. Jiang, X. B. Zhang, G. L. Shen and R. Q. Yu, *Anal. Chim. Acta*, 2007, **583**, 40.
23 L. Li and B. Li, *Analyst*, 2009, **134**, 1361.
24 H. W. Liao and J. H. Hafner, *Chem. Mater.*, 2005, **17**, 4636.
25 C. G. Wang and J. Irudayaraj, *Small*, 2008, **4**, 2204.
26 K. L. Ai, Y. L. Liu and L. H. Lu, *J. Am. Chem. Soc.*, 2009, **131**, 9496.
27 X. Liu, Q. Dai, L. Austin, J. Coutts, G. Knowles, J. H. Zou, H. Chen and Q. Huo, *J. Am. Chem. Soc.*, 2008, **130**, 2780.
28 Z. P. Li, C. H. Liu, Y. S. Fan and X. R. Duan, *Anal. Bioanal. Chem.*, 2007, **387**, 613.
29 Z. H. Sheng, H. Y. Han, D. H. Hu, J. G. Liang, Q. G. He, M. L. Jin, R. Zhou and H. C. Chen, *Chem. Commun.*, 2009, 2559.
30 Y. Q. He, S. P. Liu, L. Kong and Z. F. Liu, *Spectrochim. Acta, Part A*, 2005, **61**, 2861.